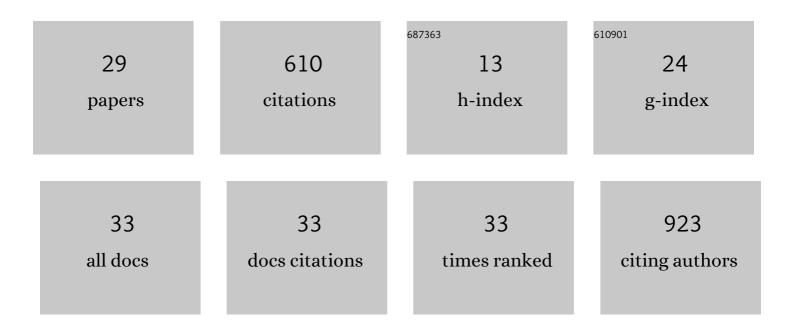
Nikola Chmel

List of Publications by Year in descending order

Source: https://exaly.com/author-pdf/3775727/publications.pdf Version: 2024-02-01



#	Article	IF	CITATIONS
1	Influence of the tetraalkoxysilane crosslinker on the properties of polysiloxane-based elastomers prepared by the Lewis acid-catalysed Piers-Rubinsztajn reaction. Polymer Chemistry, 2021, 12, 4934-4941.	3.9	4
2	Insight into the Mechanism of Action and Peptideâ€Membrane Interactions of Aibâ€Rich Peptides: Multitechnique Experimental and Theoretical Analysis. ChemBioChem, 2021, 22, 1656-1667.	2.6	11
3	Enhanced properties of well-defined polymer networks prepared by a sequential thiol-Michael - radical thiol-ene (STMRT) strategy. European Polymer Journal, 2021, 151, 110440.	5.4	5
4	Exploring the Potential of Molecular Spectroscopy for the Detection of Post-translational Modifications of a Stressed Biopharmaceutical Protein. Current Protein and Peptide Science, 2021, 22, 800-806.	1.4	1
5	SOMSpec as a General Purpose Validated Self-Organising Map Tool for Rapid Protein Secondary Structure Prediction From Infrared Absorbance Data. Frontiers in Chemistry, 2021, 9, 784625.	3.6	1
6	CD81 extracted in SMALP nanodiscs comprises two distinct protein populations within a lipid environment enriched with negatively charged headgroups. Biochimica Et Biophysica Acta - Biomembranes, 2020, 1862, 183419.	2.6	16
7	Transformation of aqueous protein attenuated total reflectance infra-red absorbance spectroscopy to transmission. QRB Discovery, 2020, 1, .	1.6	3
8	A strained alkyne-containing bipyridine reagent; synthesis, reactivity and fluorescence properties. RSC Advances, 2019, 9, 36154-36161.	3.6	3
9	Hepatic VLDL secretion: DGAT1 determines particle size but not particle number, which can be supported entirely by DGAT2. Journal of Lipid Research, 2019, 60, 111-120.	4.2	16
10	Fluorescence detected linear dichroism spectroscopy: A selective and sensitive probe for fluorophores in flowâ€oriented systems. Chirality, 2018, 30, 227-237.	2.6	7
11	Fluorescence detected linear dichroism of small molecules oriented on polyethylene film. Analyst, The, 2018, 143, 5805-5811.	3.5	8
12	Spatial positioning of EB family proteins at microtubule tips involves distinct nucleotide-dependent binding properties. Journal of Cell Science, 2018, 132, .	2.0	44
13	Light scattering corrections to linear dichroism spectroscopy for liposomes in shear flow using calcein fluorescence and modified Rayleigh-Gans-Debye-Mie scattering. Biophysical Reviews, 2018, 10, 1385-1399.	3.2	6
14	Infrared absorbance spectroscopy of aqueous proteins: Comparison of transmission and ATR data collection and analysis for secondary structure fitting. Chirality, 2018, 30, 957-965.	2.6	18
15	Multifaceted Studies of the DNA Interactions and In Vitro Cytotoxicity of Anticancer Polyaromatic Platinum(II) Complexes. Chemistry - A European Journal, 2016, 22, 8943-8954.	3.3	21
16	Membrane protein extraction and purification using styrene–maleic acid (SMA) copolymer: effect of variations in polymer structure. Biochemical Journal, 2016, 473, 4349-4360.	3.7	109
17	Redox-active and DNA-binding coordination complexes of clotrimazole. Dalton Transactions, 2015, 44, 3673-3685.	3.3	23
18	Oxidized polyethylene films for orienting polar molecules for linear dichroism spectroscopy. Analyst, The, 2014, 139, 1372-1382.	3.5	20

NIKOLA CHMEL

#	Article	IF	CITATIONS
19	Spectroscopic signatures of an Fmoc–tetrapeptide, Fmoc and fluorene. RSC Advances, 2013, 3, 10854.	3.6	22
20	Calculations of flow-induced orientation distributions for analysis of linear dichroism spectroscopy. Soft Matter, 2013, 9, 4977.	2.7	15
21	Circular and Linear Dichroism Spectroscopy for the Study of Protein–Ligand Interactions. Methods in Molecular Biology, 2013, 1008, 211-241.	0.9	11
22	Jahn–Teller effects on π-stacking and stereoselectivity in the phenylethaniminopyridine tris-chelates Cu(NN′)32+. Dalton Transactions, 2012, 41, 4477.	3.3	12
23	Considerations of Noise and Measurement Reproducibility of Circular Dichroism Measurements Using Na[Co ^{III} (EDDS)]. Chirality, 2012, 24, 699-705.	2.6	3
24	TTF salts of optically pure cobalt pyridine amidates; detection of soluble assemblies with stoichiometry corresponding to the solid state. Dalton Transactions, 2011, 40, 1722.	3.3	13
25	Chiral Semiconductor Phases: The Optically Pure D ₃ [M ^{III} (<i>S</i> SEDDS)] ₂ (D = TTF, TSF) Family. Inorganic Chemistry, 2011, 50, 4039-4046.	4.0	6
26	Origins of stereoselectivity in optically pure phenylethaniminopyridine tris-chelates M(NN′)3n+ (M =) Tj ETQq	0 0 <u>,0</u> rgBT	/Overlock 10

27	Organic-soluble optically pure anionic metal complexes PPh4[MIII(S,S-EDDS)]·2H2O (M = Fe, Co, Cr). Dalton Transactions, 2010, 39, 2919.	3.3	15
28	Self-assembling optically pure Fe(Aâ \in "B)3 chelates. Chemical Communications, 2009, , 1727.	4.1	82
29	Exploring the formation of 3D ferromagnetic cyano-bridged Cull2+x{Cull4[WV(CN)8]4–2x[WIV(CN)8]2x}·yH2O networks. Journal of Materials Chemistry, 2007, 17, 2308	6.7	34